Automated methods for efficient & accurate electroretinography

Luke T Havens[1, 3], Alexandra CN Kingston[2, 3], & Daniel I Speiser[3]

[1]UNC Department of Biology, Coker Hall, CB #3280, 120 South Road, Chapel Hill, NC 27599
[2]Department of Biological Science, Oliphant Hall Rm 304, The University of Tulsa, 800 South Tucker Drive, Tulsa, OK 74104
[3]Department of Biological Sciences, University of South Carolina, 715 Sumter Street, Columbia, SC 29208

[1]corresponding author: lukethavens@gmail.com ; +1 843 601 3199; ORCID: 0000-0002-4754-2101
Alexandra CN Kingston ORCID: 0000-0002-1982-8831
Daniel I Speiser ORCID: 0000-0001-6662-3583

Keywords: ERG, visual ecology, crayfish, spectral sensitivity, automation

Electroretinography (ERG) is a foundational method for assessing visual system physiology, but accurate ERG can be time- and labor-intensive, often involving manual adjustment of the wavelength and intensity of light stimuli and real-time comparison of physiological responses to inform those adjustments. Furthermore, current approaches to ERG often require expertise beyond that necessary for the electrophysiological preparation itself. To improve both the efficiency and accessibility of ERG, we designed an automated system for stimulus presentation and data acquisition. Here we test this novel system's ability to accurately assess spectral sensitivity in the well-characterized visual system of the crayfish *Procambarus clarkii* using three approaches: the first, based on response magnitude, maximizes efficiency; the second is a well-established method we use to further validate our efficient approach's accuracy. Third, we explore the potential benefits of extensible automation using a method assessing the interplay between temporal acuity and spectral sensitivity. Using our system, we are able to acquire accurate results in ERG experiments quickly (testing the entire visible spectrum in 8 min, 30 s using our response magnitude approach). Moreover, data collected via all three methods yielded results consistent with each other and previous work on *P. clarkii*.

Introduction

The responses of animals to their environments can be challenging to predict and interpret because different animals perceive the world in very different ways. Most animals respond to light, for example, but the visual systems of animals vary in the kind and quality of information they gather (Land & Nilsson 2012). Among other differences, the visual systems of animals vary in the wavelengths of light to which they are sensitive and the temporal rates at which they sample the surrounding light environment (Cronin et al. 2014). These physiological differences can have profound implications for behavior: for example, if an animal is better able to distinguish between wavelengths of light, it may more accurately distinguish between toxic and nontoxic prey items or better evaluate mate quality (Cuthill et al. 2017). Further, the temporal sampling rates of visual systems range from less than 1 Hz to over 250 Hz, with fast-sampling systems being better-suited for resolving fast-moving objects or scenes (Land & Nilsson 2012; Warrant 1999; Vogel 1956). It is apparent that visual ecology—the ways in which animals perceive, interpret, and interact with their visual environment—is an important factor in understanding behavior. But differences between the physiological properties of visual systems make it difficult to ask questions about the behavioral relevance of visual stimuli without first determining an organism's sensitivity to those stimuli.

Electroretinography (ERG) is a technical method used to amplify, record, and assess the electrophysiological responses of sensory structures to light stimuli. In ERG protocols, researchers vary features of light such as intensity, wavelength, and temporal dynamics to create stimuli that can be used to assess different aspects of visual performance. Importantly for this paper, ERG can be used to assess the magnitude of a sensory structure's electrophysiological response to a given light stimulus. To date, all electrophysiological methods of assessing the spectral sensitivity of a visual system are based on this concept: that response magnitude increases with the visual system's sensitivity to a particular stimulus or the intensity of that stimulus. Additionally, ERG can be used to assess the temporal acuities of visual systems by determining the fastest-resolvable flickers of stimuli, known as a system's flicker fusion frequency (FFF).

Inconveniently, simply separating a light source into spectral bands and assessing response magnitude to each, as in the first case of ERG (Waller 1900), yields inaccurate results. Light sources do not emit light equally across the spectrum and a larger response magnitude might just as easily denote greater stimulus intensity as higher sensitivity. By differentially modulating each band of light, this response magnitude method was made more accurate, though it was still criticized as only accurately characterizing a visual system's peak sensitivity (Kennedy 1961).

Eventually, the response magnitude method was supplanted by an approach known as the criterion response method, which was based on an older, psychophysical method that used pupil diameter as an inverse measure of spectral sensitivity (Wagman & Gullberg 1942). Rather than using equal-intensity stimuli, this method adjusts intensity to elicit equal-magnitude responses across the spectrum (Kennedy & Bruno 1961). The intensity required to elicit this criterion response across the spectrum is then plotted as an inverse measure of sensitivity. Because assessment of stimulus intensity can be conducted *post hoc*, the criterion response method is feasible even if generating equivalent-intensity stimuli is not. However, the criterion response method requires repeated stimulation at each tested wavelength and real-time stimulus adjustment, making it time-consuming and technically demanding. There have been efforts to automate the criterion response method, but these require purpose-built systems capable of real-time feedback of response magnitude to adjust stimulus intensity (Rocha et al. 2016; de Souza et al. 1996). Perhaps more importantly, these automated methods preclude dark adaptation--and thus measuring absolute sensitivity limits--because of their use of a constantly flickering light stimulus to elicit a consistent AC response.

This history of ERG methods development led us to posit that there may be another approach to automation not yet attempted. Specifically, we wondered if the inaccuracy of the response magnitude method may have been due to technical constraints rather than biological ones. Indeed, some researchers have drawn inspiration from the original balanced-intensity response magnitude approach to design updated methods for ERG based on converting response magnitudes to sensitivity (Telles et al. 2014; Beckmann et al. 2015). These sensitivity-converted response approaches are nearly identical to the historical response magnitude method save for

the addition of normalizing responses to stimulus intensity. The similarity between the contemporary and historical method made us question whether the sensitivity-converted response method was effective due to conceptual or technical improvements.

In addition to automating existing methods, we explored new approaches modular automation might make possible by investigating the interplay of spectral sensitivity and temporal acuity. The temporal acuity of visual systems tends to increase with light intensity, so FFF is typically reported in terms of the maximum value possible--that is, the fastest rate at which an eye can respond regardless of further increasing stimulus intensity (Warrant 1999; Warrington et al. 2017; Frank 2003). Based on this intensity dependence, we posited that temporal acuity might also vary with perceived intensity, or sensitivity. Spectral variation in temporal acuity could have implications for the sensory ecology of animals living in spectrally complex environments. As a first step to investigating this potentially complex interaction of spectral sensitivity and temporal acuity, we proposed a method that may only be feasible with a fully automated ERG system: assessing FFF to isoquantal stimuli across the visual spectrum.

In this paper, we present a system for automated ERG, including the generation and presentation of stimuli and the recording of electrophysiological responses. We describe and assess the ERG system we designed on technical grounds, including factors such as system noise level and accuracy of stimulus generation. Using this system, we assess the accuracy and efficiency of three automated ERG methods in the crayfish *Procambarus clarkii*, a species known from previous electrophysiological studies to have short wavelength-sensitive (SWS) photoreceptors, with peak sensitivities at 440 nm, whose responses are dwarfed by the responses of more numerous long wavelength-sensitive (LWS) photoreceptors, with peak sensitivities reported between 562 and 570 nm (Cummins & Goldsmith 1981; Kong & Goldsmith 1977; Kennedy & Bruno 1961). First, we assess an automated version of the response magnitude method using both dark and light adaptation to compare response curves to theoretical LWS and SWS photoreceptor sensitivities. Second, we verify the accuracy of our response magnitude method by comparison to data collected by a sensitivity-converted response method. Third, we evaluate our proposed spectrally influenced temporal acuity method. Finally, we assess our system and methods in concert for ease of use, efficiency, and extensibility.

Methods

Equipment for electrophysiology

Electrophysiological recordings were amplified by an AM Systems model 3000 AC/DC differential amplifier with headstage (Sequim, WA). All recordings were taken in DC. Our response magnitude and sensitivity-converted response methods used a low pass cutoff of 20 kHz; the spectrally influenced temporal acuity data were collected using a low pass cutoff of 3 kHz. Amplified signals were filtered by a Quest Scientific HumBug 60 Hz Noise Eliminator (North Vancouver, British Columbia) before being passed to an ADInstruments PowerLab model 8/35 data acquisition board (Colorado Springs, CO). Signals were then digitized and recorded in Labchart 8 Pro (ADInstruments). All equipment was powered by a Furman PST-8D 60 Hz power conditioner (Petaluma, CA).

Recordings were taken on a passively isolated air table with attached breadboard (ThorLabs SDH7512 & B3048F; Newton, NJ). Fine scale electrode placement was accomplished using Narishige MM-3 manual micromanipulators (Amityville, NY). The work area was completely enclosed by a custom-built Faraday cage composed of electrically insulated layers of ferritic steel and copper with its interior painted matte black. An extension of the Faraday cage that was shielded both from the surroundings and the work area served as a shelf for the amplifier, HumBug, and data acquisition board.

Equipment for generating and manipulating light

Light generation was separated into two functions: generation of monochromatic light for test stimuli and generation of band- and long-pass light for adapting stimuli. Although separate physically, these systems were controlled in tandem (Figure 1). In the system used to generate light for test stimuli, broad spectrum light was provided by a Spectral Products 150 W tungsten-halogen lamp (ASBN-W150-PV) and separated into monochromatic light stimuli using a Spectral Products CM110 monochromator (Putnam, CT). Light from the lamp-monochromator assembly was focused onto a 1mm core optical fiber using an F-number matching fiber adapter

(Spectral Products SF1000-SMSM-U20-MAJ-MC-050-HT & AF-CMDK-L). Light exiting the optical fiber was collimated using an achromatic doublet lens (ThorLabs AC060-010-A-ML) into a light control assembly that consisted of a Uniblitz LS3 high-speed shutter (Rochester, NY) and a continuously variable, circular neutral density filter (Edmund Optics 54-082; Barrington, NJ) affixed to a high-precision servo motor (Dynamixel MX-64R; Robotis, Lake Forest, CA). After exiting the control assembly, light was refocused onto the first of the split ends of a bifurcated fiber optic cable using an achromatic doublet lens (ThorLabs BFY1000HS02 & AC060-010-A-ML).

In the system used to generate light for adapting stimuli, broad spectrum light was provided by a 20 W tungsten-halogen lamp with an integrated shutter (Ocean Optics HL-2000-HP-FHSA; Dunedin, FL). Light was collected by a 1 mm core optical fiber (Spectral Products SF1000-SMSM-U20-MAJ-MC-050-HT); after exiting the optical fiber, light was collimated into a filter assembly using an achromatic doublet lens (ThorLabs AC060-010-A-ML). In the filter assembly, light was projected through a filter wheel containing 480, 520, and 570 nm bandpass filters and a 600 nm longpass filter (Thorlabs FB480-10, FB520-10, FB570-10, FEL0600). Light was then projected through a continuously variable, circular neutral density filter (Edmund Optics 54-082) attached to a high precision servo motor (Dynamixel MX-64R) and refocused onto the second of the split ends of the bifurcated optic cable using an achromatic doublet lens (ThorLabs BFY1000HS02 & AC060-010-A-ML).

The bifurcated cable, carrying both signals, was passed into the Faraday cage and the common end was used as the light source for experiments. In cases where light adaptation was not necessary, a doublet achromatic lens was used to collimate the output and lessen the effect of distance on the irradiance received by the test preparation.

Assessment of light output

Light received by test preparations was quantified as absolute irradiance at a distance (~1 cm) and orientation similar to that of the electrophysiological preparations. Absolute irradiance (integrated from 375 to 725 nm) was measured using a spectrometer system with components from Ocean Optics, including a Flame-S-VIS-NIR-ES spectrometer, a QP400-1-UV-VIS optical

fiber, and a CC-3 cosine-corrector. The absolute spectral response of the spectrometer was calibrated using a HL-3P-CAL Vis-NIR calibrated light source and the spectrometer was operated using Ocean View software.

ERG automation

A Raspberry Pi 3 model B (RasPi) was used to communicate with and control the various components of the light generation system described above. The RasPi was modified to identify and initialize communication with the bandpass filter wheel, monochromator, Ocean Optics integrated shutter, and the motors controlling the positions of the two continuously variable circular neutral density filters (Figure 1). The monochromator was connected to the RasPi via a USB-RS232 adapter (StarTech ICUSB232V2; Lockbourne, OH); the neutral density filter motors were connected via a USB-RS485 adapter (JBTek BC22164; Surrey, BC, Canada). The RasPi also served as a library for data on the light output of the system and as a repository of wavelength-specific transmission measurements of the neutral density filters. This stored information was used to automatically calculate the positions of the two circular neutral density filters required to achieve the desired irradiance of the test stimuli and adapting stimuli. All operations on the RasPi were completed in Python 2.7.

Communication with the RasPi occurred through a connection between the GPIO pins of the RasPi and the digital in/out of the PowerLab data acquisition board. The two systems communicated through custom-written 8 bit commands, as well as the use of two bytes in succession to achieve 16 bit integer resolution as needed. This communication was controlled in LabChart through a series of macros written in VBScript. In addition to light control, these systems automatically recorded all changes made to light output in the LabChart document at the time of change.

Users can choose between two approaches to system control: writing custom protocols from existing components or following macro-generated prompts. Basic system control macros were written and named to make them easily accessible as modular blocks that can be combined into custom code. For example, these basic control macros can be used to change output wavelength or intensity of light from either the monochromator or bandpass filter systems, run

the high-speed shutter at chosen frequencies, or present a series of stimuli with chosen period, interstimulus period, and irradiance parameters. By combining these basic control macros, users can create code for custom experimental protocols that, by nature of its readability, accurately documents protocols for review and re-use. Alternatively, users without programming experience (or not in need of custom protocols) can follow prompts generated by macros accessible via a drop-down menu. These prompts can be used to access all of the basic functionalities of the system, such as those mentioned before. In addition, all of the experimental protocols presented in this paper can be initiated by following simple prompts defining experimental parameters (such as stimulus, interstimulus, and adaptation periods, as well as stimulus and adaptation wavelengths and irradiance) generated by a single macro. This allows users to define and run long-form, automated experiments without any coding experience.

Animal care & preparation

Feeder crayfish (*Procambarus clarkii*, approximately 15-60 mm) were procured from Carolina Biological Supply Company (Burlington, NC) and housed in a 15 gallon glass aquarium prior to use in recordings. To prepare them for ERG, crayfish were anesthetized on ice and affixed to a post by wrapping in Parafilm (Bemis NA, Neenah, WI). The grounding electrode was placed in the abdomen and the reference and recording electrodes were placed in the non-illuminated and illuminated eyes, respectively. Electrodes were uncoated, electrolytically sharpened tungsten rods.

Response magnitude method

The response magnitude approach to ERG consisted of two components: trials and adaptation periods. Each trial consisted of a randomly ordered presentation of 31 monochromatic, irradiance-balanced test stimuli spaced every 10 nm from 400-700 nm. Test stimuli were presented in a pattern of 1 s on, 10 s off, where the off period consisted of only the adaptation condition. Trials, therefore, can be viewed as the functional units of the modular response magnitude method. Adaptation periods were 20 minutes of the adaptation condition: either bandpass light or darkness. Appropriate periods for stimulus presentation, rest, and

adaptation were determined by preliminary experiments. Adaptation conditions were kept constant throughout the entire adaptation period and subsequent trial.

Test animals (*P. clarkii*) were subjected to a total of four trials, with two trials presented in a state of maintained dark adaptation and two trials presented in a state of maintained light adaptation. In the light-adaptation trials, light was filtered through a 570 nm bandpass filter and presented at an irradiance of 1.75×10^{14} photons/cm^2/s. Trials were presented in the pattern of dark-light-dark-light so that crayfish had two dark and two light adaptation periods. Monochromatic stimuli were presented at an irradiance of 1.75×10^{13} photons/cm^2/s. Appropriate irradiance values were determined by preliminary experiments. Responses to stimuli in each trial were assessed for magnitude, defined as maximum deflection from resting voltage. To compare between animals, responses were normalized using the equation $N = 10^{(lnR - lnR_{max})}$, where R is the response magnitude to be converted, R_{max} is the maximal response magnitude in the spectral series, and N is the normalized response. The result was a normalized series distributed between 0 and 1. Normalized responses to the same wavelength in trials of the same condition (either dark or light) were averaged together to produce a mean normalized response for each condition and wavelength in each animal.

Sensitivity-converted response method

Our approach here was nearly identical to our response magnitude method, except that this method used response curves to stimuli of the same wavelength but varying intensity as a reference for relating response magnitudes in a spectral series to each other and calculating sensitivity. This approach normalized and linearized relationships between sigmoidally varying response magnitudes by relating each response to the logarithmic irradiance required to elicit it. As in our response magnitude method, trials consisted of 31 isoquantal, monochromatic stimuli presented in random order in the pattern of 1 s on, 10 s off. Prior to each trial, crayfish were adapted for 20 minutes to either darkness or 570 nm bandpass light. For these experiments, the stimulus light was presented at an irradiance of 6.00×10^{13} photons/cm^2/s and the adapting light was presented at an irradiance of 6.00×10^{14} photons/cm^2/s.

Unlike our response magnitude method, trials in this method were bookended by the collection of response in voltage versus logarithmic stimulus intensity (*V*log*I*) curves generated by presenting 570 nm light in 15 irradiance values increasing from 3×10^{11} to 4.63×10^{14} photons/cm^2/s logarithmically in a pattern of 1 s on, 10 s off. After the *V*log*I* run preceding each trial, animals were given 10 minutes to readjust to the adaptation conditions of the trial. For data interpretation, sigmoidal curves were fit to both the pre- and post- *V*log*I* curves using a least-squares approach in custom-written Python 3.6 code. Response magnitudes to trial stimuli were converted to sensitivity using the formula $S = 10^{(logI_{eq} - logI_{max})}$, where I_{eq} is the irradiance within the *V*log*I* curve causing an equivalent response to that being converted, I_{max} is the irradiance within the *V*log*I* curve causing an equivalent response to the maximum response within the spectral series, and *S* is sensitivity (Telles et al. 2014). Sensitivity was calculated for each stimulus using both pre- and post-trial *V*log*I* curves. These values were combined so that the first response in the series used only sensitivity calculated from the pre-trial *V*log*I* curve, the last used only the post-trial calculation, and the relative contribution of each sensitivity calculation varied smoothly for the responses recorded in-between. This was done to account for any changes to the preparation over the course of the experiment.

Spectrally influenced temporal acuity method

Our spectrally influenced temporal acuity method was based on the phenomenon of visual systems demonstrating increased temporal acuity with increased irradiance (Frank 2003; Warrington et al. 2017). From this, we posited that visual systems' temporal acuities would similarly vary with wavelength-specific sensitivity to a given stimulus. In order to test this hypothesis, our approach determined FFF to isoquantal, monochromatic stimuli. Each preparation experienced a single irradiance across the test spectrum. Across all test animals, this irradiance ranged from 3.0 - 5.1 $\times 10^{13}$ photons/cm^2/s over the course of long-term data collection. Test animals (*P. clarkii*) were allowed to dark adapt for 20 minutes before being presented with monochromatic test stimuli in random order spaced every 10 nm in the range of 400-700 nm. At each wavelength, the stimulus flickered at a range of frequencies from 3-49 Hz (increasing by one hertz each step) in a pattern of 2 s flickering, 2 s dark. In one case where it

was clear that FFF exceeded 49 Hz at one or more wavelengths, stimuli flickering at frequencies of 50-54 Hz were presented at the end of the normal protocol in a pattern of 2 s on, 2 min off to avoid shutter damage. All flicker trains were controlled via the high-speed shutter being run by a square wave pulse. After recordings were complete, crayfish were visually assessed for FFF to each monochromatic stimulus by a researcher blind to the wavelength being assessed (Frank 2003, McComb et al. 2010). FFF for a given stimulus was defined as the highest frequency the eyes of a crayfish followed; we scored a stimulus as being followed if response peaks remained in phase with the flickering stimulus for either ten flashes in a row or the entire stimulus period.

Visual pigment curve fitting & statistical analyses

We fit visual pigment absorption curves to our interpreted data (either normalized or sensitivity-converted) using a custom-written least squares approach in Python 3.6. Visual pigment absorption curves were modeled as described by Stavenga (2010). All other statistical analyses were also performed in Python 3.6.

Results

Electrophysiology equipment, stimulus generation, & automation

The intrinsic noise of the system was approximately 7 μV peak-peak (2 μV rms) with a voltage drift of approximately 9 μV per minute. The use of the Humbug Noise Eliminator had no impact on these figures. Light output of our unmodified lamp-monochromator assembly varied by greater than an order of magnitude. By using our automated system, we reduced this variation in output to within 10% of any specified irradiance across the system's output spectrum (400-700 nm; see figure 2). We determined this level of accuracy to be stable for approximately 10 days, after which the deterioration of the bulb had progressed enough for desired and actual output irradiance to differ by more than 10%. By re-assessing light output via a system-guided spectrometer protocol that automatically incorporated new measurements into lamp output libraries, we were able to again reduce the variance between desired and actual output intensity to less than 10%. Communication between the user interface, RasPi, and downstream

components had a high degree of fidelity: we observed no miscommunication between these devices.

Response magnitude method

Using our response magnitude method, we found that the eyes of dark-adapted *P. clarkii* had a λ_{max} of 567 ± 4 nm; after adapting eyes with 570 nm bandpass light, their λ_{max} shifted to 438 ± 6 nm (Figure 3a). Moreover, our results were not dependent on the use of multiple trials for each preparation—calculating λ_{max} from a single trial of each adaptation condition in each animal did not have a significant effect on the values of λ_{max} that were calculated. To assess the necessity of trial-averaging to this method's accuracy and allow comparison to single-trial methods, results from this method were arbitrarily limited to the first trial of both dark- and light-adaptation. This limited dataset yielded a dark-adapted λ_{max} at 563 ± 6 nm and a light-adapted λ_{max} at 439 ± 7 nm, neither of which were significantly different from results using trial-averaging (ANOVA; dark-adapted $p = 0.09$, light-adapted $p = 0.76$).

Trials using our response magnitude method took a total of 8 min 30 s, allowing multiple trials per animal. The total regimen, including four trials (2 dark, 2 light) and four 20 min adaptation periods to either dark or 570 nm light took 2 hrs. Automation was successful for the duration of these experiments.

Sensitivity-converted response method

Using our automated version of the sensitivity-converted response method, we calculated a λ_{max} of 562 ± 7 nm for eyes of dark-adapted animals and a λ_{max} of 467 ± 69 nm for eyes of light-adapted animals (Figure 3b). Results in dark-adapted animals were not significantly different from those from our response magnitude method arbitrarily trial-limited for statistical comparison between these separate approaches (ANOVA; $p = 0.57$). Results from light-adapted animals were omitted from comparison to data collected via other methods due to some animals in this group showing equivalent λ_{max} before and after light adaptation and the resulting high spread of peak sensitivity.

Sensitivity conversion itself had no significant effect on λ_{max} values calculated for results from our sensitivity-converted response method. If data were treated identically to the response magnitude method—that is, if responses were not converted to sensitivity using the *V*log*I* curves we collected and were instead simply normalized—we calculated dark-adapted λ_{max} at 562 ± 7 nm and light-adapted λ_{max} at 464 ± 74 nm (Figure 3c). These values were not significantly different from those generated using sensitivity-converted data (ANOVA; dark-adapted $p = 0.83$, light-adapted $p = 0.91$).

Trials of our automated sensitivity-converted response method took a total of 28 minutes, discounting light or dark adaptation prior to beginning the trial. The total regimen of one dark and one light trial with associated 20-minute adaptation periods took 96 minutes. Automation was successful for the entire experimental regime.

Spectrally influenced temporal acuity method

Data from our spectrally influenced temporal acuity method showed a λ_{max} consistent with the other methods we tested. Fitting visual pigment absorption curves following the same procedure as for our response magnitude method (normalization followed by least-squares curve fitting) yielded a λ_{max} at 565 ± 11 nm (Figure 3d). This was not significantly different from the results in dark-adapted animals using our previous methods (ANOVA; single-trial response magnitude $p = 0.68$; sensitivity-converted response $p = 0.47$). Testing 47 frequencies (3-49 Hz in steps of 1 Hz) at 31 wavelengths (400-700 nm in steps of 10 nm) took 90 minutes, and automation was successful for the entire long-form experiment.

Discussion

Spectral sensitivity and temporal acuity have profound impacts on the kind and quality of information available to an animal about its visual environment. Understanding visual systems on this physiological level allows us to ask more informed questions about the behavioral responses of animals to their surroundings. ERG can be used to probe these physiological

questions, and therefore should be understood as a foundational technique in understanding an animal's visual ecology.

Our work demonstrates that ERG, like many other foundational methods with long histories, should be continually updated with the advent of new technology. We were able to automate our three approaches to ERG, vastly improving efficiency: using our response magnitude method, we recorded an entire spectral response series in 8 min, 30 s. In comparison to what can be a lengthy, manual process this is a major improvement. In addition to lowering the time cost of ERG, high-efficiency methods are uniquely suited to time- or sample-limited preparations. For example, higher efficiency can allow more exhaustive testing procedures in endangered animals which cannot be subjected to lengthy electrophysiology preparations for the sake of their well-being or a higher number of technical replicates in sample-limited animals such as those from the deep sea (Frank 2003).

Moreover, despite the fact that only one of our tested methods is currently an accepted approach to assessing spectral sensitivity using ERG, all three provided results consistent with each other and with previous work in *P. clarkii*. Previous work has reported the λ_{max} of *P. clarkii* LWS receptors between 562 and 570 nm (Kong & Goldsmith 1977; Kennedy & Bruno 1961). In comparison, our single-trial response magnitude method calculated a λ_{max} of 563 ± 6 nm, our sensitivity-converted response method calculated a λ_{max} of 562 ± 7 nm, and our spectrally influenced temporal acuity method calculated a λ_{max} of 565 ± 11 nm. This high degree of consistency between results acquired using disparate methods suggests that we were correct in our assessment that the standard protocols for ERG exist largely for historical—rather than technical—reasons.

Electrophysiology equipment

A first concern with automating any system is whether data can be collected under stable conditions over time. Automation removes the ability to modulate when data are recorded and, thus, the automation of an unstable system can quickly become a liability rather than a benefit. We succeeded in designing a low noise, low drift electrophysiology rig capable of running for extended periods of time without user intervention. Interestingly, we found that shielding and

mains conditioning were sufficient to achieve this without any kind of filtering (including smart filtering such as with a HumBug Noise Eliminator). Potential users, however, should keep in mind that while equipment noise is a ceiling beyond which recording quality cannot improve, limiting biological noise remains a necessary step of developing any electrophysiological preparation. Still, having found that this system has lower noise levels in total than some electrophysiological amplifiers have on their own, we can recommend the design of this rig independently from the methods we built it to test.

Stimulus generation & automation

Similar to the stability of electrophysiological equipment, the stability and fidelity of digital communication is paramount when creating an automated system. If communication between system components were to break down or be misinterpreted, animals could be subjected to the wrong stimulus without the user's knowledge. However, we found no evidence of this when testing our rig.

Although the ultimate test of whether irradiance values are sufficiently balanced is their effectiveness for accurate ERG recordings, the reduction in variability between wavelengths is striking.We report irradiance values as within 10% of our target values and it appears a large proportion of the variation is due to temporal fluctuation in the intensity of the lamp. Since optical density filters remove a proportion of the light rather than a constant amount, fluctuation at the light source will be proportional to fluctuation in the irradiance experienced by preparations. In other words, we believe our accuracy of stimulus presentation may begin to approach the physical limit of the system. This, along with the difficulty of manually filtering wavelengths differentially to the degree that we have done, lends credence to our presumption that previous iterations of the response magnitude method may have been limited by technical—rather than biological—factors.

We took great efforts to maintain the modularity and extensibility of our automated system. Even the methods we describe in this paper ask the user to define experimental parameters. Though we used consistent test parameters for our protocols described here, when a user begins a new experiment, they are prompted to define features such as test wavelengths,

stimulus and interstimulus periods, and adaptation periods and conditions. Should other researchers wish to use our automated system with nocturnal animals, for instance, it would require no extra steps for them to use shorter stimulus periods and longer interstimulus and adaptation periods than those we utilized in our work on *P. clarkii*. In addition to the modularity of the methods we present in this paper, all of the base functionalities of our ERG system are accessible via readable VBScript commands (e.g. 'set_mono_wavelength()' and 'open_bandpass_shutter()' for controlling the monochromator and bandpass light systems, respectively). Users can string these commands together to make entirely novel automated ERG protocols or add features to existing protocols, such as a test flash presented between stimuli for assessing the adaptation state of an eye. This means that the potential applications of our automated ERG system far exceed those we present here.

Response magnitude method

Our automated response magnitude method for ERG yielded results consistent with those previously obtained in *P. clarkii* with a high degree of efficiency. Moreover, repeated trials of the same adaptation condition within a single animal did not improve the accuracy of λ_{max} calculations, suggesting repeated trials could be avoided in the case of extremely time-limited preparations where λ_{max} was the primary feature of interest. Especially given its single-trial accuracy, this method represents our maximum-efficiency approach, one that may be uniquely suited for the sorts of time- or sample-limited preparations discussed earlier. It should also be noted that we chose our stimulus and inter-stimulus periods to suit our study animal; shorter periods are commonly used in ERG experiments and can be performed by our system. That is, our stated trial time (8 min, 30 s)—while much faster than most ERG methods—is relatively arbitrary and underestimates the potential efficiency of our system and approach.

Since our response magnitude method is particularly efficient, we wanted to give any potential future users further insight into the process of using it to study novel visual systems. As with any ERG protocol, the first step is developing a viable preparation, including limiting any biological noise and verifying recording stability. For our method, the preparation development stage also entails determining appropriate experimental parameters, such as stimulus,

interstimulus, and adaptation periods, as well as the irradiance values for stimulus and adaptation conditions. For example, as in our ERG experiments on previously uncharacterized visual systems (Kingston et al. 2019), we identified a stimulus intensity, stimulus period, and interstimulus period that elicited responses across the test spectrum without saturating responses at any wavelengths or affecting responses to subsequent stimuli. This is determined easily using a sparse sampling of the test spectrum via our automated method, varying parameters as necessary. In our experience, this process takes no more time than normal preparation development—during which response characteristics would already be tested—and is greatly aided by taking what is known of the animal's visual ecology into account (diurnal vs. nocturnal, for instance). After data collection, in uncharacterized visual systems it is also often appropriate to test whether stimulus response curves are best explained by multiple photopigments, exceptional tools for which have already been developed (Lessios 2017).

Sensitivity-converted response method

We further validated the accuracy of our automated response magnitude method using an automated version of a currently accepted method for assessing spectral sensitivity using ERG based on sensitivity conversion (Telles et al. 2014; Beckmann et al. 2015). In doing so, we found that not only was our response magnitude method sufficient to assess spectral sensitivity accurately, but that sensitivity conversion and our approach to normalization did not have meaningfully different effects on our estimates of λ_{max}. This method and our response magnitude method did not yield statistically different calculations of dark-adapted λ_{max}. Moreover, there was no appreciable difference in result whether data collected via this method were converted to sensitivity or simply normalized as in our automated response magnitude method. It would seem that in the context of carefully controlled experiments, converting responses to sensitivity rather than simply normalizing them amounts to a distinction without a difference. Additionally, because our normalization function does not account for stimulus order, randomized stimulus presentation successfully mitigated any spectrally consistent effects of preparation change over time that can manifest in ordered presentation paradigms. Potential users should note, however, that determining appropriate adaptation and interstimulus periods is paramount when not

correcting for or assessing changes in adaptational state. Still, given the extra time cost of collecting data for the sensitivity-converted response method (28 min per trial vs. 8 min 30 s in the response magnitude method), we found our response magnitude method enhanced efficiency without sacrificing accuracy.

We designed our normalization formula explicitly with replacing sensitivity conversion in mind. Since the potential of any electrochemical cell varies with the natural logarithm of its ion concentrations, the cell's responses to stimuli should scale with the natural logarithm as well (Nernst 1889; Goldman 1943). Instead of relating response to irradiance—a relationship that scales with log base-10—we normalized responses on this natural logarithm scale and achieved results similar to those obtained by sensitivity conversion (Figure 3c). Sensitivity-converted data yielded a λ_{max} of 562 ± 7 nm; the same data when normalized yielded a λ_{max} of 562 ± 7 nm. Given these indistinguishable results, we suggest that our normalization method effectively yields the same amount of information as sensitivity conversion without linearizing the sigmoidal response curves of photoreceptors.

Spectrally influenced temporal acuity method

Our temporal acuity method was designed to demonstrate the new questions in visual ecology that can be asked with an automated and programmable ERG system. To the best of our knowledge, this represents the first systematic investigation of the relationship between the spectral sensitivity and temporal acuity of a visual system. Interestingly, even this relationship followed the general pattern of our results, yielding a λ_{max} consistent with our other measures of the crayfish LWS receptor. However, this method did not detect the crayfish's SWS receptor. While this might be expected in additive, magnitude-based measures, FFF is a non-additive measure. If one population of photoreceptors follows a stimulus while another population does not, a recording from both should show the stimulus being followed: fluctuation added to a flat line looks like fluctuation. In this context, the relatively straightforward relationship we saw between wavelength and FFF in the visual system of *P. clarkii* belies how unpredictable the relationship between wavelength and FFF might be across species, even those in which the λ_{max} values of photoreceptors are already known.

Assessing relationships between spectral sensitivity and temporal acuity is a fruitful avenue for future research in visual ecology. This interplay could have implications for behavior, such as influencing the speeds at which animals can maintain optic flow while moving through environments of different spectral qualities or the scanning speeds that animals can use while distinguishing spectrally cryptic objects. Moreover, this method demonstrates the value of an automated system in developing new approaches to ERG. Even in cases where rapid stimulation would not lead to undue light adaptation, presenting nearly 1500 unique stimuli to the eyes of a single animal might easily take longer than the viability of the preparation without the high level of automation for ERG we have achieved.

Conclusion

Despite the importance of ERG in understanding the visual capabilities of animals, its technical difficulty has limited the scope of its application. After reviewing the history of its development, we set out to design a more accessible and efficient approach to ERG. We found our system to be easier to teach and use than others with which we are familiar. Whereas common ERG techniques (such as the criterion response method) might require hours of labor from an expert, our technique can assess the responses of a visual system to the visible spectrum of light in less than ten minutes and requires minimal training to operate. We hope that these improvements in efficiency and accessibility open the door for more researchers to use ERG in their studies of visual systems.

To ensure that other researchers are able to benefit from our work, we've made the code running our ERG system entirely open-source [insert link]. This code and our system are designed to be modular and extensible so that others are able to modify the system to work with their existing equipment or easily define new methods and protocols appropriate for work with animals from different habitats or with dissimilar visual systems. We look forward to seeing the unexpected ways in which others expand on our system and protocols for ERG.

Declarations

Author contributions

LTH designed and built the electroretinography apparatus, conceived of and programmed the automated electroretinography protocols, and collected spectrally influenced temporal acuity & sensitivity-converted response data. ACNK collected response magnitude data. DIS oversaw the project. All authors contributed to analyzing data and drafting the manuscript.

Funding

Support for the authors was provided, in part, by IOS Award no. 1457148 from the National Science Foundation (to DIS), as well as a Magellan Scholar Award from the University of South Carolina and a Science Undergraduate Research Fellowship from the South Carolina Honors College (both to LTH).

Code availability

All code involved in the automated ERG system is open-source and can be found at [insert link]. Code performing common functions such as visual pigment curve fitting and statistical analyses are available from the corresponding author, LTH, upon reasonable request.

Conflicts of interest

The authors declare no conflicts of interest.

Ethics approval

We followed all applicable rules and regulations for the care of crustaceans in the United States.

Consent to participate

Not applicable.

Consent for publication

Not applicable.

Availability of data & material

The data that support the findings of this study are available from the corresponding author, LTH, upon reasonable request.

Acknowledgements

For their advice on this project, the authors thank Christine Bedore and Dan Chappell. LTH also thanks Dick Vogt for initial training in the field of electrophysiology.

Literature Cited

Beckmann H, Hering L, Henze MJ, Kelber A, Stevenson PA, and Mayer G (2015) Spectral sensitivity in *Onchyophora* (velvet worms), phototactic behaviour and opsin gene expression. *J Exp Biol* 218:915-922

Cronin TW, Johnsen S, Marshall J, and Warrant EJ (2014) *Visual Ecology*. Princeton University Press, Princeton, NJ

Cummins D and Goldsmith TH (1981) Cellular identification of the violet receptor in the crayfish eye. *J Comp Physiol* 142:199–202

Cuthill IC, Allen WL, Arbuckle K, Caspers B, Chapelin G, Hauber ME, Hill GE, Jablonski NG, Jiggins CD, Kelber A, Mappes J, Marshall, J, Merrill R, Osorio D, Prum R, Roberts NW, Roulin A, Rowland HM, Sherratt TN, Skelhorn J, Speed MP, Stevens M, Stoddard MC, Stuart-fox D, Talas L, Tibbetts E, and Caro T (2017) The biology of color. *Science* 357(6350)

de Souza JM, Devoe RD, Schoeps C, and Ventura DF (1996) An AC constant-response method for electrophysiological measurements of spectral sensitivity functions. *J Neurosci Methods* 68:203–210

Frank TM (2003) Effects of light adaptation on the temporal resolution of deep-sea crustaceans. *Integr Comp Biol*, 43(4):559–570

Goldman DE (1943). Potential, impedance, and rectification in membranes. *J Gen Physiol*, *27*(1):37–60

Kennedy D and Bruno MS (1961) The spectral sensitivity of crayfish and lobster vision. *J Gen Physiol* 44(6):1089-1102

Kingston ACN, Lucia RL, Havens LT, Cronin TW, & Speiser DI (2019). Vision in the snapping shrimp *Alpheus heterochaelis*. *J Exp Biol* 222(21):jeb209015.

Kong K and Goldsmith TH (1977) Photosensitivity of retinular cells in white-eyed crayfish (*Procambarus clarkii*). *J Comp Physiol* 122:273–288

Land MF and Nilsson D-E (2012) *Animal Eyes*. Oxford University Press, New York, NY

Lessios N (2017) Using electroretinograms and multi-model inference to identify spectral classes of photoreceptors and relative opsin expression levels. *PeerJ* 5:e3595.

McComb DM, Frank TM, Hueter RE, & Kajiura SM (2010). Temporal resolution and spectral sensitivity of the visual system of three coastal shark species from different light environments. *Physiol and biochem zool* 83(2):299–307.

Nernst W (1889) Die elektromotorische Wirksamkeit der Jonen. *Zeitschrift Für Physikalische Chemie* 4U(1):129-181

Rocha FA, Gomes BD, Silveira LC, Martins SL, Aguiar RG, de Souza JM, and Ventura DF (2016) Spectral sensitivity measured with electroretinogram using a constant response method. *PloS one* 11(1)

Stavenga DG (2010) On visual pigment templates and the spectral shape of invertebrate rhodopsins and metarhodopsins. *J Comp Physiol A* 196(11):869-78

Telles FJ, Lind O, Henze MJ, Rodríguez-Gironés MA, Goyret J, and Kelber A (2014) Out of the blue: the spectral sensitivity of hummingbird hawkmoths. *J Comp Physiol A* 200:537-546

Vogel G (1956) Verhaltensphysiologische Untersuchungen über die den Weibehenbesprung des Stubenfliegen-Männchens (*Musca domestica*) auslösenden optischen Faktoren. *Zeitschrift Für Tierpsychologie* 14(3):309–323.

Wagman IH and Gullberg JE (1942) The relationship between monochromatic light and pupil diameter. The low intensity visibility curve as measured by pupillary measurements. *Am J Physiol* 137(4):769-78

Waller AD (1900) On the retinal currents of the frog's eye, excited by light and excited electrically. *Phil Trans B* 193:123-63

Warrant EJ (1999) Seeing better at night: life style, eye design and the optimum strategy of spatial and temporal summation. *Vision Research* 39(9):1611-30

Warrington RE, Hart NS, Potter IC, Collin SP, and Hemmi JM (2017) Retinal temporal resolution and contrast sensitivity in the parasitic lamprey *Mordacia mordax* and its non-parasitic derivative *Mordacia praecox*. *J Exp Biol* 220:1245-55

Figures

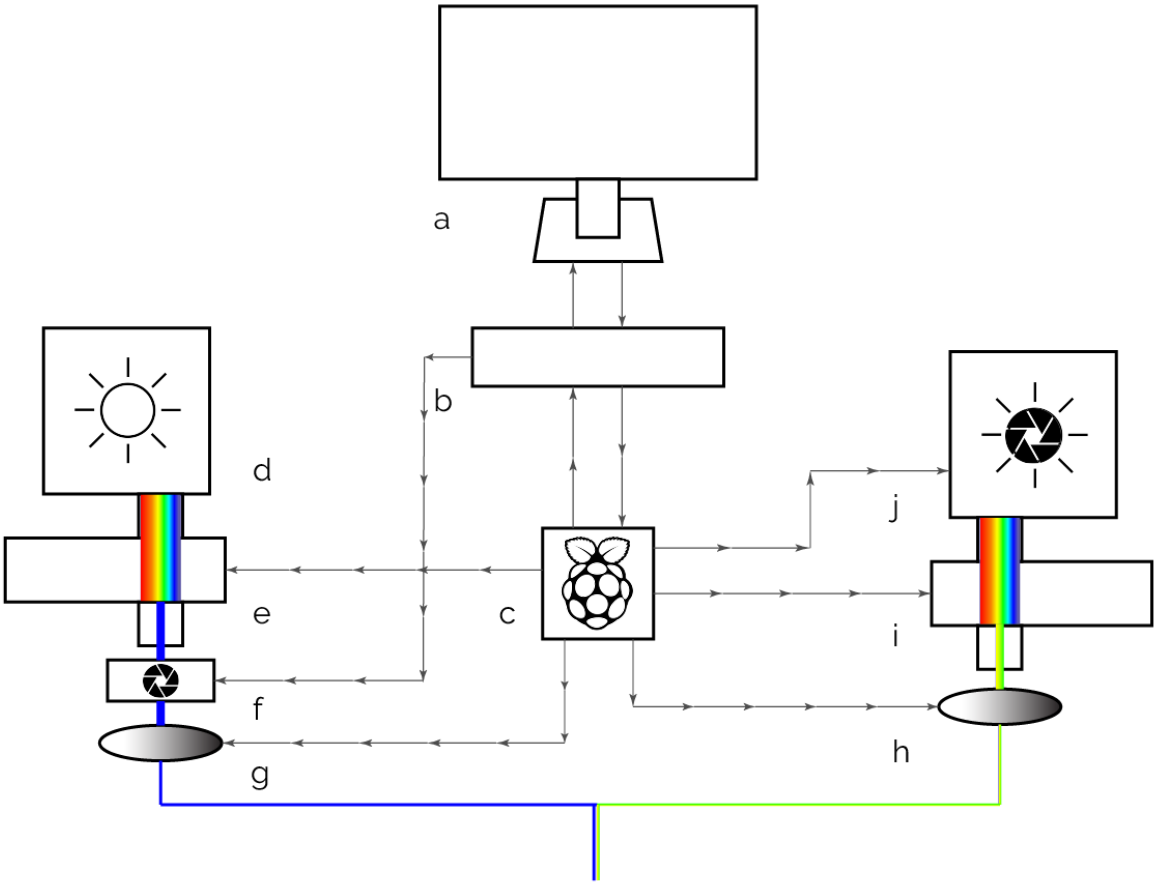

Fig. 1 Block diagram of the stimulus generation apparatus of the automated ERG showing light generation and connectivity with direction of control. Briefly, the left-hand system generates monochromatic stimuli while the right-hand system generates bandpass adapting light. The majority of the system is controlled via the RasPi, while the high-speed shutter is run via the data acquisition board. Labels are as follows: **a** Graphical User Interface: lab computer running Windows 10; **b** data acquisition board; **c** Raspberry Pi microcomputer; **d** 150 W lamp; **e** monochromator; **f** high-speed shutter; **g, h** Continuously variable neutral density wheels and controlling motors; **i** Bandpass filter wheel; **j** integrated lamp and shutter

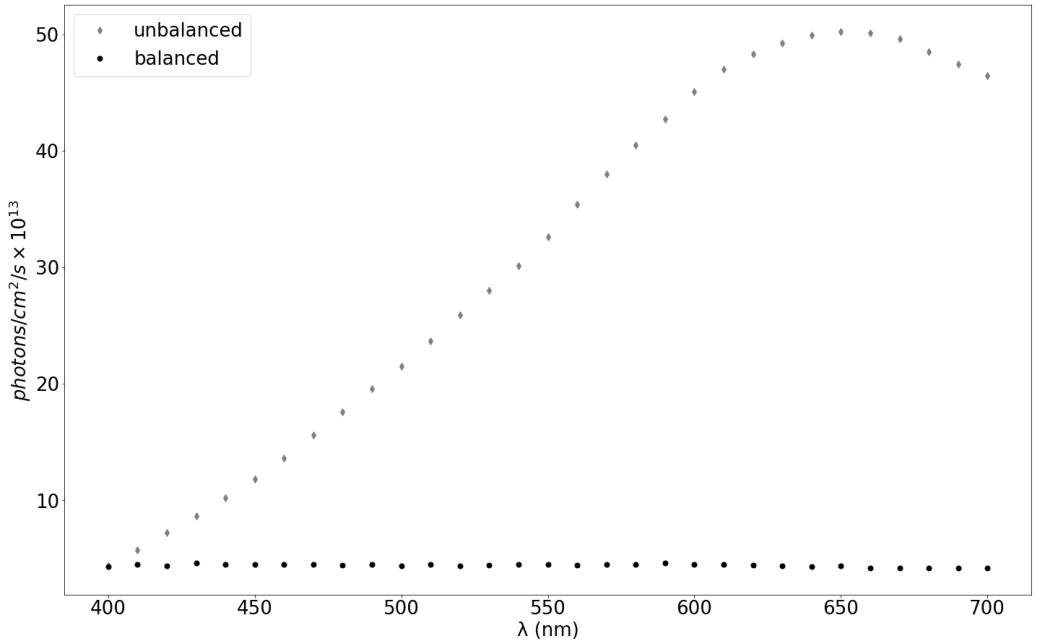

Fig. 2 Representative irradiance values associated with unbalanced (gray) and balanced (black) light output from the lamp-monochromator assembly. Irradiance associated with the unbalanced output varies by greater than an order of magnitude, whereas irradiance associated with the balanced output (balanced, in this case, to the lowest unbalanced output) varies by less than 10% across the range of wavelengths tested

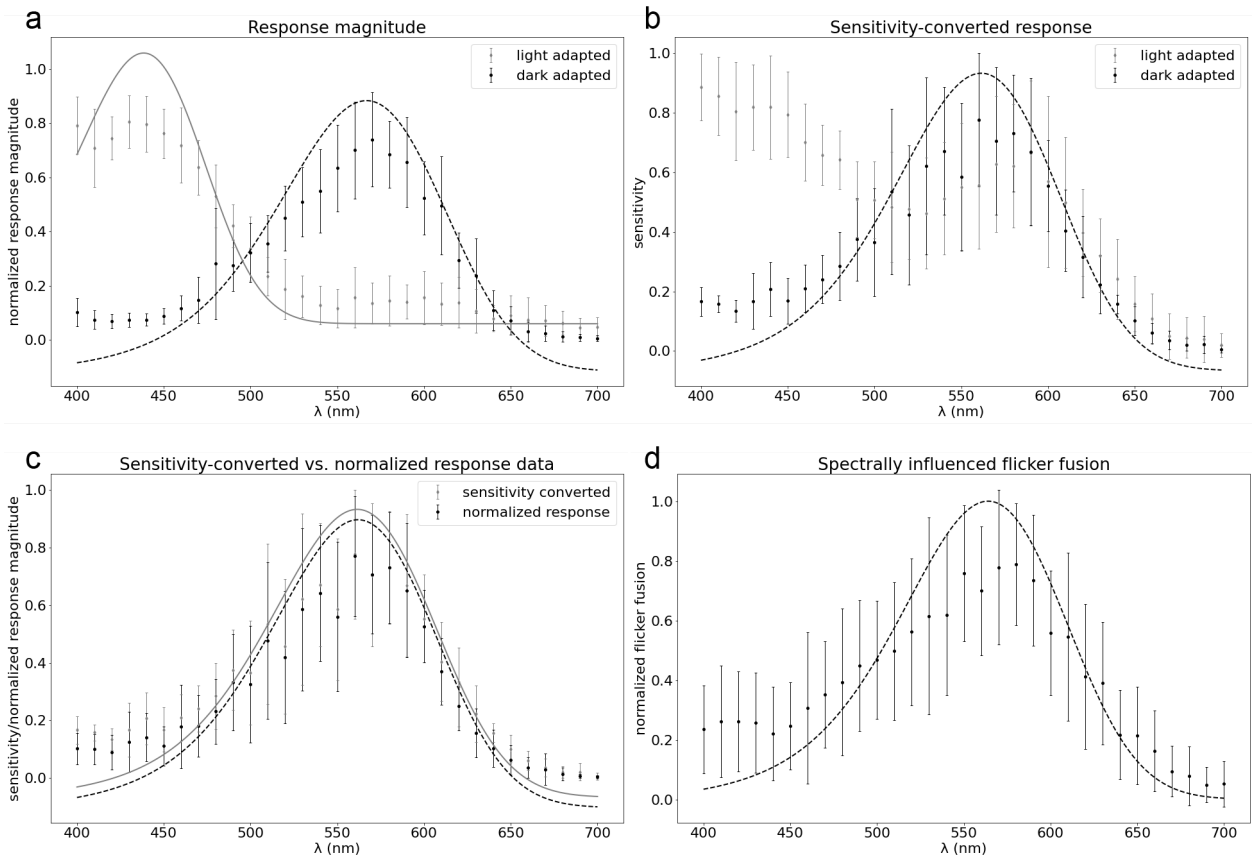

Fig. 3 ERG data from our various methods; error bars show standard deviation. Each method provided results consistent with each other and with previous work in *P. clarkii*. **a** Data from our response magnitude method. Gray points show data from trials after adaptation to 570 nm light (λ_{max} = 438 ± 6 nm), with the gray solid line showing a visual pigment curve fit to the data using a least-squares approach. Black points and dashed line similarly show data and fitted curve from trials after dark adaptation (λ_{max} = 567 ± 4 nm). **b** Data from our sensitivity-converted response method laid out in the same way as data from our response magnitude method (dark adapted λ_{max} = 562 ± 7 nm; light adapted λ_{max} = 467 ± 69 nm). The light-adapted visual pigment curve is omitted here because the curve fitted to the mean data did not correspond to the mean λ_{max} calculated from curve-fitting to each individual's sensitivity. **c** Dark-adapted data from our sensitivity-converted response method plotted either after sensitivity conversion (gray) or normalization (black). Sensitivity-converted λ_{max} was 562 ± 7 nm; normalized λ_{max} was 562 ± 7 nm. Values of λ_{max} were not statistically different (ANOVA; $p = 0.83$). **d** Data from our spectrally influenced temporal acuity method normalized as in our response magnitude method showing a

fitted visual pigment template with a peak corresponding with those shown in the dark-adapted cases of our other methods (λ_{max} = 565 ± 11 nm)